Trapping thresholds in invasion percolation

Lincoln Paterson
Australian Petroleum Cooperative Research Centre, CSIRO Division of Petroleum Resources, P.O. Box 3000, Glen Waverley, Vic 3150, Australia

Adrian P. Sheppard and Mark A. Knackstedt
Department of Applied Mathematics, Research School of Physical Sciences and Engineering, Australian National University, Canberra ACT 0200, Australia
and School of Petroleum Engineering, University of New South Wales, Sydney, NSW 2052, Australia
(Received 9 July 2002; published 21 November 2002)

We give numerical estimates for the site percolation trapping thresholds for invasion percolation on various three dimensional lattices. We find that in most cases the thresholds for invasion and ordinary percolation coincide. However, for coordination numbers less than five the thresholds diverge. Since most rock networks exhibit coordination numbers less than five the rules for simulating residual saturation in porous rocks must be chosen carefully.

DOI: 10.1103/PhysRevE.66.056122 PACS number(s): 64.60.Ak, 47.55.Mh

I. INTRODUCTION

Percolation theory is useful to explain trapped residual fluids in petroleum reservoirs [1,2] and groundwater hydrology [3]. In the language of percolation theory ''the fraction of sites occupied'' can be mapped to measurement of fluid saturation (fraction of the pore space occupied by a fluid phase). Within this context of multiphase flow in porous media, percolation theory has been applied in several variants, both as ordinary percolation and invasion percolation, and with and without trapping rules. A description of percolation with trapping can be found in several textbooks [4–8].

There seems to be general consensus that slow ''drainage'' (displacement of a wetting fluid by a nonwetting fluid in slow capillary dominated displacements in porous media) is well described by invasion percolation with trapping (TIP). Note that here ''wetting'' is used in the physicochemical sense, which is different from some of the usage in percolation where ''wetting'' is used to label the introduced phase [9].

The correct rules for ''imbibition'' (displacement of a nonwetting fluid by a wetting fluid) are still being debated [10,11], and probably depend on rate and the contribution of flow in thin films. Both *ordinary* percolation and *invasion* percolation with trapping, with variants, are candidates. If invasion percolation with trapping and ordinary percolation with trapping give the same results, then it may not matter which rule to use and the debate is academic. For example, Wilkinson and Willemsen [12] studied *invasion* percolation with trapping on the simple cubic lattice and observed an invading phase trapping threshold of $p_t \sim 0.66$. Paterson [13] studied *ordinary* percolation with trapping (TOP) on the same lattice and observed a trapping threshold of $p_t \sim 0.658$. Within the numerical uncertainty these values are identical, supporting the notion that the choice of model is not significant.

The mean coordination number $\overline{z}$ or mean number of connections from each site, is an important concept in porous media. Estimates of trapping thresholds on lattices other than the simple cubic grid ($z=6$) have been neglected until recently due to the large computational effort necessary to check for trapping after each site is added. Few attempts have been made to correlate network studies to the true topology of sedimentary rock. This is despite mounting evidence that rock networks exhibit much lower coordination numbers. Ioannidis *et.al.* [14,15] measured the average coordination number $\overline{z}$ from serial sections of a sandstone core and from stochastic porous media and found $\overline{z}=3.46$ [14] and $\overline{z}\simeq 4.1$ [15], respectively. Oren and co-workers [16,17] developed a process-based reconstruction procedure which incorporates grain size distribution and other petrographical data obtained from two dimensional (2D) thin sections to build network models that are analogues of real sandstones. The average coordination number derived from the resultant pore network is $\overline{z}=3.5$ [17]. Direct measurement of a 3D pore structure via synchrotron x-ray computed microtomography (micro-CT) [18] coupled with skeletonization algorithms [19] has allowed groups to directly measure the pore coordination number in rock networks; results indicate that $\overline{z}\leqslant 4.0$ for most sandstones. Lindquist *et al.* [20] derived the topological properties of a suite of Fontainebleau sandstone samples with porosity varying from 7.5% to 22%. The average coordination number varied from $\overline{z}=3.37$ at $\phi=7.5\%$ to $\overline{z}=3.75$ at $\phi=22\%$. All measurements imply that the coordination number of the network is significantly less than $z=6$. These studies highlight the need to consider trapping thresholds on a range of lattices. In this paper, percolation thresholds with trapping are compared over a range of coordination numbers to see if TIP and TOP always give the same results. The conclusion is that for coordination numbers greater than or equal to five, this is the case. However, below a coordination number of five the thresholds diverge and the choice of model is significant.

II. IMPLEMENTATION

In simple ordinary site percolation, a given site of the lattice has a probability p of being present or occupied and a

corresponding probability $1-p$ of being empty or vacant. There is a critical value of p that separates the globally disconnected and globally connected states for an infinite lattice. To perform an actual realization of the percolation process, sites on a finite lattice may be preassigned values from a uniform probability distribution so that the sites occupied can be determined by choosing sites with values less than p, and unoccupied sites have values greater than p. The occupied sites are then tested to determine if they span the lattice.

In invasion percolation, at each step the site with the largest value *adjacent to the invading cluster* is chosen to be the next site to be occupied. Thus the number of sites available for growth is substantially limited, and the invading cluster is always connected. For ordinary percolation this limitation does not exist and the site with the largest value anywhere on the lattice can be chosen, so that the invading cluster is disconnected.

Trapping rules can be applied to both ordinary and invasion percolation. In both cases, regions that become completely enclosed by invading fluid become excluded from further occupancy by invading fluid. Trapping algorithms have been computationally very slow, because as each new site is invaded a search of the entire lattice to label all connected sites has been made. Recent developments by one of us (A.P.S.) has led to an optimized trapping routine [21].

Simulations are performed on $L\times L\times L$ lattices. We measure the finite threshold $p_t(L)$ for the fraction of the invading phase in two ways: when the defending fluid becomes disconnected and no longer spans the lattice from inlet to outlet (rule $\Re_1$) and second, when all the defending fluid is trapped and no further invasion is possible (rule $\Re_2$). Simulations on lattices were performed for a range of lattice sizes up to 200^3.

III. RESULTS

A. Lattices

We consider invasion percolation with trapping (TIP) on seven lattices [22]: The 12-coordinated hexagonally close packed lattice (HCP), the face-centered cubic lattice (FCC), the body-centered cubic lattice (BCC), the six-connected simple cubic lattice (SC), the four-coordinated diamond and NbO lattices [23] (Fig. 1) and the three-coordinated Y^* lattice [23] (Fig. 2).

(i) $z=12$. The data for the HCP and FCC lattices were generated on lattices up to $L=128$. Data for the HCP lattice are summarized in Fig. 3(a). Finite size scaling was used to determine the extrapolated value of $p_t(L\to\infty)$ by fitting to the relationship

$$p_t = p_t(L) - AL^{-y}. \tag{1}$$

The extrapolated values and fits to the relationship are given in Fig. 3(b) and in Table I. For ordinary percolation one finds that the exponent $y=1/\nu$ where ν is the correlation length exponent. We note that the fit to Eq. (1) is very good yet the resultant exponent y is very different from the ordinary percolation result. This deviation from $1/\nu$ has been noted previously [13,24].

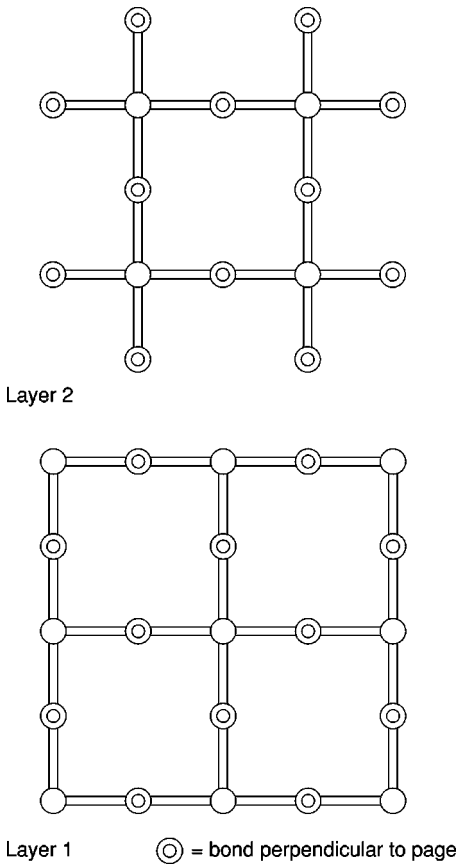

FIG. 1. NbO lattice with coordination number 4.

(ii) $z=8$. Data for the BCC lattice was generated on grids up to $L=80$. The trapping threshold and finite size scaling exponent are given in Table I.

(iii) $z=6$. This lattice has been studied extensively previously [24]. The trapping threshold and finite size scaling exponent are given in Table I.

(iv) $z=4$. Data for the diamond lattice were generated on lattices up to $L=128$. We found a good fit to Eq. (1) for the $\Re_2$ rule, but the data for the $\Re_1$ condition did not lead to a good finite size scaling fit (see Fig. 3). Values of p_t and y are summarized in Table I. Data for the NbO lattice were generated on lattices up to $L=64$.

(v) $z=3$. Each node of the three-coordinated Y^* lattice has 3 ten-rings surrounding each site. Trapping data for the

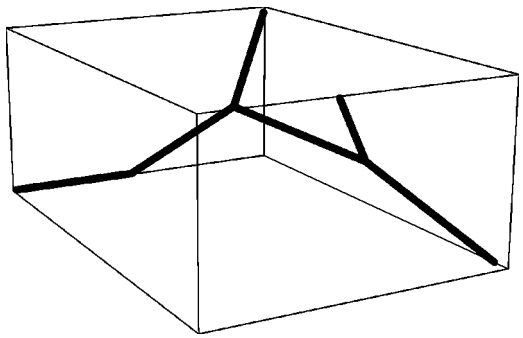

FIG. 2. Perspective view of a unit in the Y^* lattice. Adjacent vertical layers are offset.

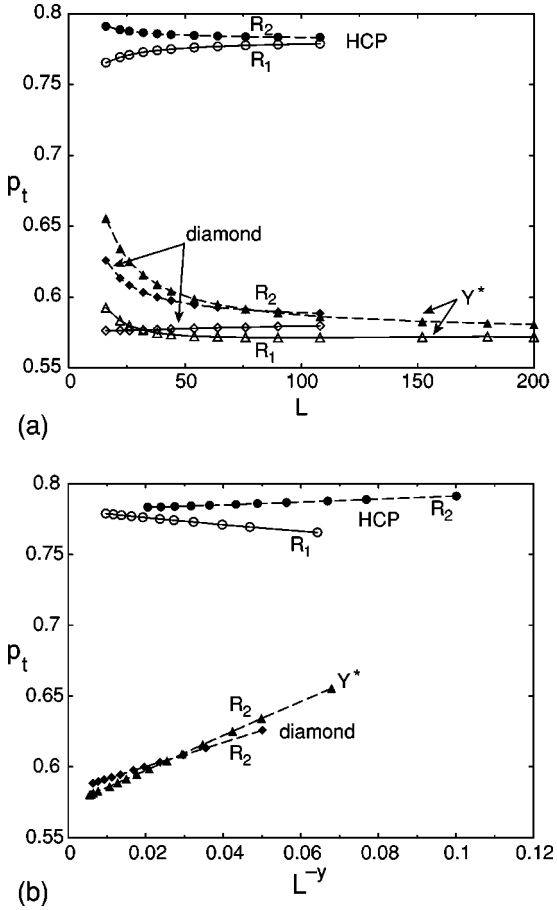

FIG. 3. Trapping thresholds $p_t(L)$ for three different lattices plotted against (a) L, and (b) L^{-y}. The HCP lattice is shown with circles, the diamond lattice is shown with diamonds, and the Y^* lattice is shown with triangles. Unfilled and filled symbols are for the $\Re_1$ and $\Re_2$ rules, respectively. The lines show the fit to Eq. (1) with p_t and y as defined in Table I.

TABLE I. Extrapolated thresholds and finite size scaling exponent for invasion percolation with trapping (TIP) on different lattices.

Lattice	z	p_t	y
HCP($\Re_1$)	12	0.7816	0.83
HCP($\Re_2$)	12	0.7821	0.99
FCC($\Re_1$)	12	0.780	0.99
FCC($\Re_2$)	12	0.782	1.25
BCC($\Re_1$)	8	0.727	1.06
BCC($\Re_2$)	8	0.729	0.87
SC($\Re_1$)	6	0.6598	0.66
SC($\Re_2$)	6	0.6599	1.21
NbO($\Re_1$)	4	0.595	0.59
NbO($\Re_2$)	4	0.593	1.17
Diamond($\Re_2$)	4	0.5830	1.08
Y^*($\Re_2$)	3	0.5734	0.97

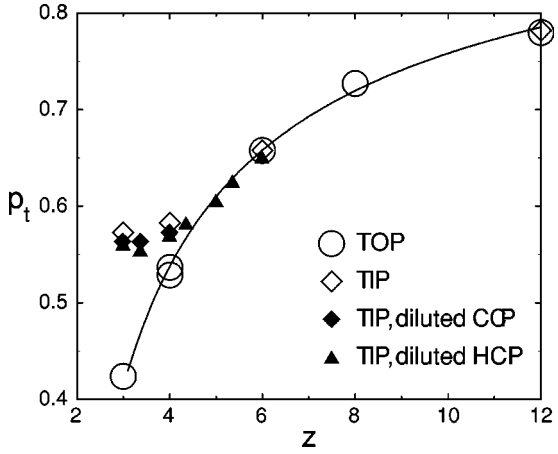

FIG. 4. Comparison of the thresholds for TOP and TIP. Circles are for TOP from Ref. [13], diamonds are for TIP on regular lattices. TIP thresholds for the diluted HCP lattice (filled triangles) and CCP lattice (filled diamonds) are also shown. The line gives the prediction of Galam and Mauger [25].

Y^* lattice were generated on lattices up to $L=214$. We find a good fit to Eq. (1) for the $\Re_2$ rule, but the data for the $\Re_1$ condition again leads to a poor fit. In fact, the $p_t(L)$ for $\Re_1$ is not monotonic and exhibits a minimum value for intermediate $L\simeq 100$. The finite size scaling fit for $\Re_2$ rule is shown in Fig. 3(b) and the values of p_t and y are summarized in Table I.

In a recent paper the trapping thresholds for TOP on a number lattices were shown [13] to follow the formula of Galam and Mauger [25]:

$$p_t = 1 - p_0[(d-1)(z-1)]^{-a}, \tag{2}$$

where d is the dimension and $p_0=1.33; a=0.59$. A comparison of this formula and the TOP data from [13] to the TIP thresholds given here are shown in Fig. 4. One observes a strong deviation from the formula for coordination numbers $z<6$. In Table II we review the thresholds and compare to the thresholds from TOP and OP. It is interesting to note that for the low coordinated lattices, the threshold for TIP is *greater* than the corresponding threshold $(1-p_c)$ for OP. This result is suprising. It has been previously argued [12]

TABLE II. Comparison of the thresholds for TIP with those of TOP from Ref. [13] and the equivalent values from OP, $(1-p_c)$. The values of p_t^{TOP} and $1-p_c$ for the Y^* lattice are derived from the formulas derived in Paterson [13] and Galam and Mauger [25], respectively.

Lattice	p_t^{TIP}	p_t^{TOP}	$1-p_c$
HCP	0.7816	0.780	0.800
FCC	0.780	0.780	0.800
BCC	0.727	0.727	0.754
SC	0.6598	0.658	0.6884
NbO	0.593	0.537	0.578
Diamond	0.5830	0.529	0.5703
Y^*	0.5734	0.432	0.550

that the sum $p_t+p_c<1$ for *all* lattices and that $p_t+p_c\to 1$ only as $z\to\infty$. This is intuitively consistent because there are always some sites which would be filled in an OP simulation which never become available to the invading phase since they are contained inside trapped defender clusters. As z increases this trapping becomes more difficult as there are more outlets for the potentially trapped defender to escape.

B. Acceptance profile

To investigate this anomalous behavior in the observed sum $p_t^{TIP}+p_c^{OP}>1$ on lower coordinated lattices, we consider the acceptance profile $a(r)$ [12] of the cluster, which is the number of random numbers in the interval $[r,r+dr]$ which are accepted into the cluster expressed as a fraction of the total number of random numbers available within the interval. Defining the normalized acceptance profile $a(x)$ where $x\in[0,1]$ by

$$x=\frac{\int_r^{r_{max}} a(r)dr}{\int_{r_{min}}^{r_{max}} a(r)dr} \tag{3}$$

gives the ranking of the sites independent of the distribution of values chosen at each site.

Following Wilkinson and Willemsen [12] we define the following quantities:

$$A_1(x)=\int_0^x (1-a(x'))dx', \tag{4}$$

$$A_2(x)=\int_x^1 (a(x'))dx', \tag{5}$$

which are, respectively, the probability that a random number below $x\in[0,1]$ is not chosen and a random number above $x\in[0,1]$ is chosen. We also define

$$x_{min}=\sup[x;A_1(x)\to 0 \ \text{ as } \ L\to\infty], \tag{6}$$

$$x_{max}=\inf[x;A_2(x)\to 0 \ \text{ as } \ L\to\infty]. \tag{7}$$

In ordinary percolation, the profile $a(x)$ is a trivial step function; all small random numbers $x\leqslant 1-p_c$ are accepted and all larger values rejected ($x_{min}=x_{max}=1-p_c$). The acceptance profile for TIP on the cubic lattice is shown in Fig. 5. As $L\to\infty$, the profile does not approach a step function and $x_{min}=0$. This reflects the finite probability that any random number can be trapped before it is itself invaded. A cutoff value of $x_{max}\simeq 0.6884$ is determined by requiring the best possible fit to a power law $A_2\simeq L^{-\mu}$ [12]. As predicted in Ref. [12] $x_{max}=1-p_c$; the trapping rule does not force the invader to occupy larger random numbers than it would for ordinary percolation. It will however invade up to $1-p_c$ in order to reach the threshold of the defending fluid.

In Fig. 5 we also illustrate the acceptance profile for TIP on the diamond lattices with $z<6$. This plot shows very strong differences to the results on the cubic grid. First, the probability of trapping the most favorable invasion sites is significant. Second, the value of x_{max} is significantly larger than the value of $1-p_c$. The trapping rule for the lower coordinated grid is forcing the invading fluid to enter sites with larger random numbers than it would for an ordinary percolation system. The Y^* lattice was also studied with similar outcomes to the diamond lattice. Values of x_{max} for all three lattices studied are summarized in Table III.

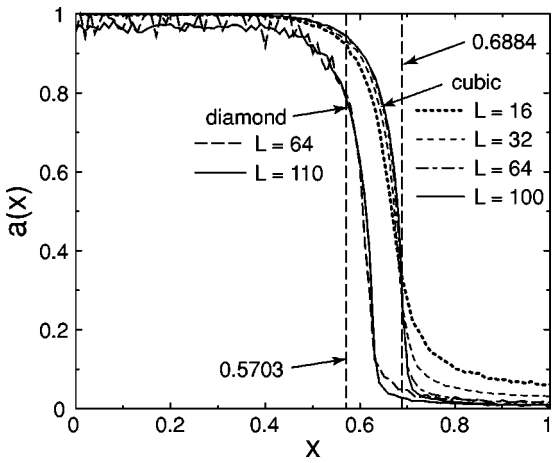

FIG. 5. Acceptance profiles for the cubic and diamond lattices. The vertical lines denote the threshold of the defender in OP, $1-p_c=0.6884$ for the cubic and $1-p_c=0.5703$ for the diamond. Note for the cubic lattice that as $L\to\infty$ the area A_2 vanishes indicating $x_{max}=1-p_c$ while A_1 remains finite, whereas for the diamond lattice $x_{max}>1-p_c$.

IV. SIMULATIONS ON DILUTED NETWORKS

The TIP and TOP thresholds begin to diverge between $4<z<6$. As we know of no five-coordinated lattice in 3D, defining a more precise range becomes problematic. We therefore, have developed a method that can be precisely controlled and allow us to consider a wider range of coordination numbers. The method we have implemented is summarized by the following 4 part algorithm [26].

(i) Construct a 12-connected network based on either a hexagonal close or a cubic close packing of spheres. In principle any network with a high coordination number could be used as a starting point.

(ii) Assign a coordination number to each site using values drawn from the specified coordination number distribution. Only z values between 3 and 11 can be generated. For a network of uniform z assign the same value to each site.

TABLE III. Comparison of the cutoff x_{max} to $1-p_c$ for three lattices. The value of p_c for the Y^* lattice is derived from the formula of Galam and Mauger [25].

Lattice	x_{max}	$1-p_c$
SC	0.6884	0.6884
Diamond	0.633	0.5703
Y^*	0.683	0.550

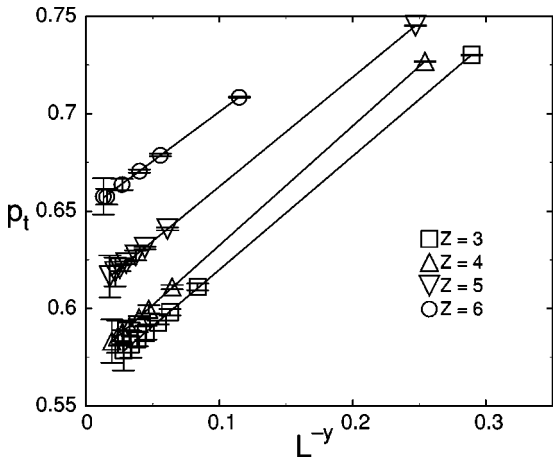

FIG. 6. Finite size scaling of the thresholds for different z diluted off the HCP lattice. In all cases the fit to scaling is excellent.

(iii) Add bonds to the diluted network one by one until, with the exception of inconsistencies, all desired coordinations have been obtained.

(iv) Build the diluted network which contains only the bonds declared to be needed during stage (iii).

The key part of the algorithm is stage (iii). At the beginning, all bonds are declared gray. During the dilution, bonds chosen to be part of the diluted network are colored white; rejected bonds are colored black.

The gray bonds are kept in a list, sorted according to priority. The priority function for the bond b connecting the sites s_1 and s_2 is

$$p_b = \frac{1}{1+F(s_1)F(s_2)}, \tag{8}$$

where the filling factor $F(s)=1-n_s/f_s$ and n_s is the number of bonds that the site still requires, while f_s is the number of gray bonds still connected to the site. For example, a site of desired coordination 6 with 2 bonds already declared white needs 4 more bonds and has 10 free bonds.

This priority function is the proportional reduction in the degrees of freedom on the subnetwork consisting of s_1, s_2 and their immediate neighbors that would result if the bond b was declared to be part of the diluted network. Selecting a bond reduces the degrees of freedom available to the network. The algorithm chooses the bond insertions that cause the smallest reduction in the number of degrees of freedom.

At each step, the bond with the maximum priority is chosen and colored white. The number of bonds needed and free on the adjacent sites are changed and then the priorities of the neighboring bonds are shifted. If a site is filled completely, then all its gray bonds are colored black and removed from the priority list. This algorithm allows us to generate stochastic networks for diluted lattices with a specific coordination number. The execution time for N_b bonds required and M bonds initially on the network is $N_b \ln(M)$. Compared to our IP simulation, which scales as $N_s \ln(n)$ where N_s is the number of sites in the network and n is the number of sites at the interface [21,27] we find the network generation is a factor of 5–10 times slower than the TIP simulation. As the network generation code is markedly slower and requires more memory we limit the study to lattice sizes at a maximum of 90^3.

TABLE IV. Extrapolated thresholds p_t and finite size scaling exponent y for stochastic diluted HCP and CCP networks along with the threshold for corresponding undiluted lattices $p_t^{lattice}$. The undiluted lattices are: $z=3$, Y^*; $z=4$, diamond; $z=6$, SC. As there is not an undiluted lattice with $z=5$ the value for $p_t^{lattice}(z=5)$ was estimated from Galam and Mauger's formula.

z	p_t^{HCP}	y^{HCP}	p_t^{CCP}	y^{CCP}	$p_t^{lattice}$
3	0.562	0.894	0.565	1.30	0.573
4	0.571	0.968	0.574	1.39	0.583
5	0.606	0.993	0.610	1.41	0.610
6	0.648	0.979	0.656	1.40	0.6598

Results

We first consider integral z and generate stochastic networks with z in the range from 3 to 6 diluted from both the HCP and the CCP lattices. The values at $z=3$, 4, and 6 can be compared to the values obtained on the regular lattices described in the previous section, and $z=5$ will allow us to investigate further where TIP and TOP diverge. Data are given in Fig. 6. The scaling of the data is in all cases excellent and the values of p_t and y are summarized in Table IV. We note that the values of p_t for the stochastic networks are consistently $\simeq 0.01$ less than the corresponding thresholds on the lattices.

We also consider systems with a range of nonintegral z. To obtain a system with noninteger z we generate a stochastic network with a fraction f of the sites $z=n$ and $(1-f)$ of the sites $z=n+1$. We generated a number of networks with nonintegral z in the range $3<z<6$. Again the fit to Eq. (1) is in all cases very good. The results are summarized in Fig. 4 where we plot all the TIP predictions, the TOP predictions from [13] and show the formula of Galam and Mauger [25]. The results indicate that the thresholds begin to diverge below $z=5$.

V. DISCUSSION

These results are significant because of the application to the prediction of residual phases in multiphase flow through porous media. The importance of coordination number on thresholds at lower z is particularly notable as recent measurements [14–17,20,26] indicate that the coordination number in equivalent network models of sandstones ranges from 3.2–4. The divergence of the thresholds for TIP and TOP at this range of z highlights the importance of choosing the correct rule for imbibition (TIP or TOP) when modeling fluid imbibition into many porous rocks. For rocks with $z>5$ the choice of modeling rules is not significant, but unfortunately this type of rock may be in a minority fraction.

[1] R.G. Larson, L.E. Scriven, and H.T. Davis, Nature (London) **268**, 409 (1977).
[2] L. Paterson, S. Painter, X. Zhang, and W.V. Pinczewski, SPEJ **3**, 211 (1998).
[3] B. Berkowitz and I. Balberg, Water Resour. Res. **29**, 775 (1993).
[4] J. Feder, *Fractals* (Plenum, New York, 1988).
[5] D. Stauffer and A. Aharony, *Introduction to Percolation Theory*, 2nd ed. (Taylor & Francis, London, 1994).
[6] M. Sahimi, *Applications of Percolation Theory* (Taylor & Francis, London, 1994).
[7] M. Sahimi, *Flow and Transport in Porous Media and Fractured Rock* (VCH, Weinheim, 1995).
[8] P. Meakin, *Fractals, Scaling and Growth Far From Equilibrium* (Cambridge University Press, Cambridge, 1998).
[9] B.D. Hughes, *Random Walks and Random Environments* (Clarendon Press, Oxford, 1996), Vol. 2.
[10] M. Blunt, M.J. King, and H. Scher, Phys. Rev. A **46**, 7680 (1992).
[11] M.J. Blunt and H. Scher, Phys. Rev. E **52**, 6387 (1995).
[12] D. Wilkinson and J.F. Willemsen, J. Phys. A **16**, 3365 (1983).
[13] L. Paterson, Phys. Rev. E **58**, 7137 (1998).
[14] M.A. Ioannidis *et al.*, SPE Paper No. 38713, 1997 (unpublished).
[15] M.A. Ioannidis and I. Chatzis, J. Colloid Interface Sci. **229**, 323 (2000).
[16] P.E. Øren, S. Bakke, and O.J. Arntzen, SPEJ **3**, 324 (1998).
[17] P.E. Øren and S. Bakke, Transp. Porous Media **46**, 311 (2002).
[18] P. Spanne *et al.*, Phys. Rev. Lett. **73**, 2001 (1994).
[19] J.F. Thovert, J. Salles, and P.M. Adler, J. Microsc. **170**, 65 (1993).
[20] W.B. Lindquist, A. Venkatarangan, J. Dunsmuir, and T.F. Wong, J. Geophys. Res., [Atmos.] **105**, 21 509 (2000).
[21] A.P. Sheppard, M.A. Knackstedt, W.V. Pinczewski, and M. Sahimi, J. Phys. A **32**, L521 (1999).
[22] A.F. Wells, *Three-dimensional Nets and Polyhedra* (Wiley-Interscience, New York, 1977).
[23] M. O'Keeffe and B.G. Hyde, *Crystal Structures: I. Patterns and Symmetry* (Mineralogical Society of America, Washington, D.C., 1996).
[24] M.A. Knackstedt *et al.*, Transp. Porous Media **44**, 465 (2001).
[25] S. Galam and A. Mauger, Phys. Rev. E **53**, 2177 (1996).
[26] R.M. Sok *et al.*, Transp. Porous Media **46**, 345 (2002).
[27] M.A. Knackstedt, M. Sahimi, and A.P. Sheppard, Phys. Rev. E **61**, 4920 (2000).